Proc. Natl. Acad. Sci. USA
Vol. 84, pp. 5937–5941, August 1987
Medical Sciences

Astrocyte gene expression in Creutzfeldt–Jakob disease

(glial fibrillary acidic protein/gene regulation/spongiform changes)

LAURA MANUELIDIS, DAVID M. TESIN, THEODOROS SKLAVIADIS, AND ELIAS E. MANUELIDIS

Yale University School of Medicine, 333 Cedar Street, New Haven, CT 06510

Communicated by Edward A. Adelberg, May 8, 1987

ABSTRACT **Gliosis (hyperplasia and hypertrophy of astrocytes), the fundamental response of the central nervous system to tissue destruction, typically becomes apparent only several weeks after injury. The biochemical hallmark of this response is a marked accumulation of the specific astrocyte intermediate filament glial fibrillary acidic protein (GFAP). To date despite its importance, the mechanisms of GFAP gene regulation have not been studied in any developmental or pathological system to our knowledge, and the molecular signals for GFAP mRNA and protein accumulation are not defined. In Creutzfeldt–Jakob disease, a progressive dementing illness caused by an "unconventional agent," we find steadily increasing elevations of GFAP mRNA throughout the later stages of disease, using two independent GFAP cDNA clones, representing the entire insert or the 3′-noncoding region (pScr-1). The accumulation of GFAP, assessed immunocytochemically, follows GFAP mRNA elevation. A 5-fold stimulation of GFAP gene expression precedes the development of florid histologic lesions in the cerebrum, and in the cerebellum 5- to 6-fold increases occurred with no detectable spongiform changes at any time during disease. Therefore, these GFAP changes cannot be simply a response to neuronal damage. These effects are directly or indirectly caused by high local concentrations of agent and possibly involve a humoral factor.**

Although the "unconventional" infectious agent (1, 2) that causes human Creutzfeldt–Jakob disease (CJD) is present in several tissues, such as spleen (3) and blood (4), it replicates to its highest titers in the brain, and only at this site are pathological changes evident. Rodents inoculated intracerebrally with high titers of the human CJD agent show minimal histological changes during the first 100 days after infection, but characteristic spongiform changes become obvious in later phases of disease (5). It is notable that the characteristic spongiform changes of CJD in the central nervous system may not be detectable in highly infectious brain samples (3), and indeed one human case of CJD transmitted to rodents showed only gliosis with no spongiform changes (6). In addition, lymphocytic infiltrates seen in most conventional viral infections are not detectable in CJD.

It was of interest to determine whether glial fibrillary acidic protein (GFAP) mRNA steady-state levels were altered in regions of brain that show essentially no spongiform or obvious pathological changes. In the hamster model of CJD, the most marked changes occur in the cerebral cortex. We therefore separated cerebellar samples (where histological disease is not apparent) from lesion-rich cerebral samples prior to RNA isolation and characterization. In addition, if GFAP mRNA levels were elevated before pathological changes occurred, GFAP could represent an effect that is induced by the agent rather than one that is elicited by secondary neuronal degeneration. Thus we analyzed RNA from brains at several time points during disease incubation, i.e., prior to the onset of clinical symptoms (99 days after inoculation), at the earliest signs of clinical disease (111 days after inoculation), and when clinical signs become definitive (122 days after inoculation). Moribund animals at terminal stages of disease (133 days) were also sampled.

The publication costs of this article were defrayed in part by page charge payment. This article must therefore be hereby marked "*advertisement*" in accordance with 18 U.S.C. §1734 solely to indicate this fact.

MATERIALS AND METHODS

Seventy-five hamsters (serial passage 18) were inoculated intracerebrally with 50 μl of rodent-passaged human CJD agent (7). Animals were sacrificed for both RNA preparations and for parallel histological studies at the selected time points. All nonsacrificed animals (n = 56) were moribund by 133 ± 1.2 days (mean ± SEM). Cerebral and cerebellar RNA samples at each time point were derived from two brains and pooled. RNA isolated from cerebrum and cerebellum CJD hamster passages 11–16 were also analyzed. RNA was isolated as described (8), and both CJD and control brain preparations yielded ≈1 mg/g of brain. RNA gel blots contained RNA from formaldehyde/agarose gels that had been electrophoretically transferred at 75–100 V for 2 hr at 4°C in 5 mM Tris acetate/1 mM EDTA, pH 7.8. Probes were labeled by replacement synthesis (9) to 10^9 cpm/μg, and hybridizations were done in 50% (vol/vol) formamide, 10% (wt/vol) dextran sulfate, 4× SSC, 2× Denhardt's solution, 20 mM sodium phosphate (pH 6.8) with extensive post-hybridization 0.1× SSC washes at 55°C prior to autoradiography. (1× SSC = 0.15 M NaCl/0.015 M sodium citrate, pH 7.0; 1× Denhardt's solution = 0.02% polyvinylpyrrolidone/0.02% Ficoll/0.02% bovine serum albumin.) Southern blots (10) were similarly hybridized. Brain regions were assayed for infectivity as described (11).

RESULTS AND DISCUSSION

Slot blots of total RNA consistently showed increased amounts of GFAP message during the later stages of CJD in all samples tested. RNA from cerebrum taken at terminal stages of CJD (≥130 days after inoculation) showed the highest elevation of GFAP mRNA levels, with >12-fold increases over normal samples. These changes were assessed more precisely with RNA gel blots.

Representative RNA gel blots of cerebrum or cerebellum RNA hybridized with a cDNA from the 3′-noncoding region of GFAP (pScr-1, *vide infra* for map) showed a single hybridizing band of 3.4 kDa (Fig. 1 *A* and *C*). This is in reasonable agreement with estimates of 3.7 kilobases (kb) for Scr-1 mRNA in scrapie-infected hamster brain (12). This hamster GFAP mRNA band is somewhat larger than a 2.7-kb mRNA reported in mouse and could be due to species differences. Inspection shows an obvious increase in Scr-1 band intensity that indicates a reasonably rapid increase in GFAP mRNA levels in both the cerebrum (Fig. 1) and in cerebellum (Fig. 1*C*, lanes 2–4) during later stages of disease

Abbreviations: CJD, Creutzfeldt–Jakob disease; GFAP, glial fibrillary acidic protein.

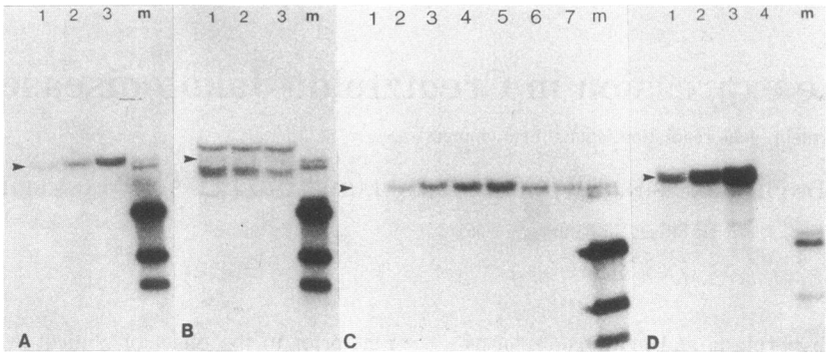

FIG. 1. RNA gel blots of brain RNA hybridized to Scr-1, neurofilament, and GFAP probes. (*A*) Cerebrum RNA from CJD passage 18 (10 μg per lane) hybridized to ^{32}P-labeled Scr-1 cDNA. Lanes: 1, 99 days after CJD inoculation; 2, 111 days; 3, 122 days with progressive increase in intensity of a 3.4-kb mRNA band at arrowhead; m, markers. (*B*) Blot A stripped of probe at 92°C in 0.1× SSC/0.5% $NaDodSO_4$ and hybridized to ^{32}P-labeled neurofilament cDNA. Comparable intensities of neurofilament mRNA bands are seen in each sample. (*C*) Cerebellar and other cerebrum preparations hybridized to pScr-1. Lanes: 1, control RNA; 2–4, CJD cerebellar RNA (10 μg each) from passage 18 taken at 99 days (lane 2), at 111 days (lane 3), and at 122 days (lane 4); 5, cerebrum RNA (passage 18) at 111 days (10 μg) shows comparable band intensity as cerebellar 122 day sample; 6, terminal CJD cerebral RNA sample from passage 11 loaded with same amount of RNA (2 μg) as control RNA in lane 1; 7, 3.5 μg of cerebellar RNA derived from terminally ill animals (passage 11). ^{32}P-labeled neurofilament cDNA hybridization and densitometry (data not shown) confirmed nominal loads, and bands detected were equivalent to *B*. (*D*) Fresh blot of cerebral CJD RNA samples (as in *A*, lanes 1–3) hybridized to ^{32}P-labeled GFAP cDNA shows comparable size and increasing intensity as detected with the Scr-1 probe. Lane 4 loaded with 2 μg of control RNA showed faint band at longer exposures. Lanes were loaded with 25 pg (*A–C*) or with 12.5 pg (*D*) of unlabeled marker pUC8 plasmid digested with *Taq* I (fragment sizes; 1420, 820, and 379 base pairs).

(99–122 days after inoculation). To quantitate the steady-state levels of GFAP mRNA by densitometry, these RNA gel blots were stripped of probe and rehybridized with a neurofilament cDNA probe (13) to provide an internal control for normalization. This probe detected two bands, distinct from the Scr-1 band, of 4 kb and 2.5 kb in accord with descriptions of the murine neurofilament mRNA (13) (Fig. 1*B*). Neurofilament mRNA levels were comparable in all CJD samples, and terminal disease samples showed maximally a 10–20% decrease in neurofilament mRNA levels. Densitometric quantitation of cerebral GFAP mRNA (using the Scr-1 probe) normalized for the amount of neurofilament message in the same lane reproducibly revealed a 2-fold increase above uninfected, control brain at 99 days after inoculation. In the cerebrum, GFAP mRNA levels increased 5-fold over normal by day 111 after inoculation, and another 2.6-fold increase was detected between 111 and 122 days. Thus there was a total 13-fold elevation of GFAP message during this early clinical period. Cerebellar GFAP mRNA levels also increased progressively during the course of infection. This finding was somewhat unexpected because the cerebellum is free of spongiform lesions. The time course of cerebellar GFAP mRNA accumulation lagged behind that of the cerebrum by 10–14 days. At 99 days after inoculation cerebellar Scr-1 mRNA levels were 1.3-fold above controls. At 111 days 2-fold normal levels were seen and at 122 days levels were 4.5-fold higher. Cerebellar samples at 122 days were comparable to cerebrum samples taken 11 days earlier (Fig. 1*C*, lanes 4 and 5).

The Scr-1 clone was originally isolated from a scrapie cDNA library and thought to represent a neuron-specific sequence that was elevated in scrapie and Alzheimer disease (12). Only in our preliminary studies did its usefulness as a 3′-specific GFAP probe become apparent. Fig. 1*D* shows a separate RNA gel blot of CJD RNA hybridized with a complete cDNA probe for mouse GFAP (14) that highlights the same 3.4-kb band as the Scr-1 probe. Although GFAP mRNA bands are more intense when using the longer complete cDNA probe (see relative intensities to picograms of unlabeled marker DNAs in Fig. 1 *A* and *D*) the above quantitative studies were performed with the potentially more-specific 3′ probe. The coding regions of several distinct intermediate filament mRNAs (e.g., GFAP, vimentin, and neurofilament) have been reported to contain homologous regions in low-stringency hybridization experiments; these homologies are confirmed by sequence, especially in central or α-helical regions (14). To test for possible cross-reactivity, the cloned probes were cross-hybridized under the same conditions used for RNA gel blots above (Fig. 2 *A* and *B*). Under the stringency conditions used, only pScr-1 and the full-copy GFAP clone cross-hybridized. To define the regions of homology, restriction fragments from each clone were prepared and analyzed on Southern blots (Fig. 2 *C–E*). The regions of overlap are illustrated in the restriction maps shown in Fig. 3. The identity of pScr-1 as a 3′-GFAP mRNA clone has also been independently confirmed by sequence analysis (A. Haase, personal communication). Because the full-length GFAP probe appears specific by these criteria, the quantitative time course of GFAP mRNA accumulation during the course of CJD infection was independently evaluated with this probe. There was an identical progressive increase in cerebral GFAP mRNA beginning at approximately day 99 and increasing to levels of >12-fold by day 122 (e.g., Fig. 1*D*).

Neuropathological assessment of astroglial hyperplasia indicated <2-fold increase in astrocytic nuclei during this phase of disease. Independent analyses of hyperplasia by autoradiography as described (15) showed that [^{3}H]thymidine only very rarely labeled astroglial nuclei during the period when GFAP mRNA was increasing. Therefore, astroglial proliferation cannot account for the mRNA elevations observed; microglial cells in the brain parenchyma that were phagocytic were labeled with [^{3}H]thymidine (data not shown). Similar results have been found in scrapie (16).

The expected consequence of the observed elevation in GFAP mRNA would be an increase in GFAP. We used immunocytochemical detection methods for detailed studies because they do not entail potential fractionation artifacts and yield valuable information in regions that may vary pathologically. Immunological detection of GFAP showed a progressive increase in the protein product within astrocytes in the later stages of disease. In some regions of the brain the massively accumulated GFAP filled enlarged astrocyte cell bodies and processes that closely apposed neuronal perikarya and dendrites (Fig. 4*B*). This observation explains the apparent *in situ* hybridization of the Scr-1 clone to neurons using frozen sections (12), which have limited resolution. Similarly, the hybridization of pScr-1 to neuritic plaques in Alzheimer disease is explained because these plaques contain many GFAP-rich astrocytic processes.

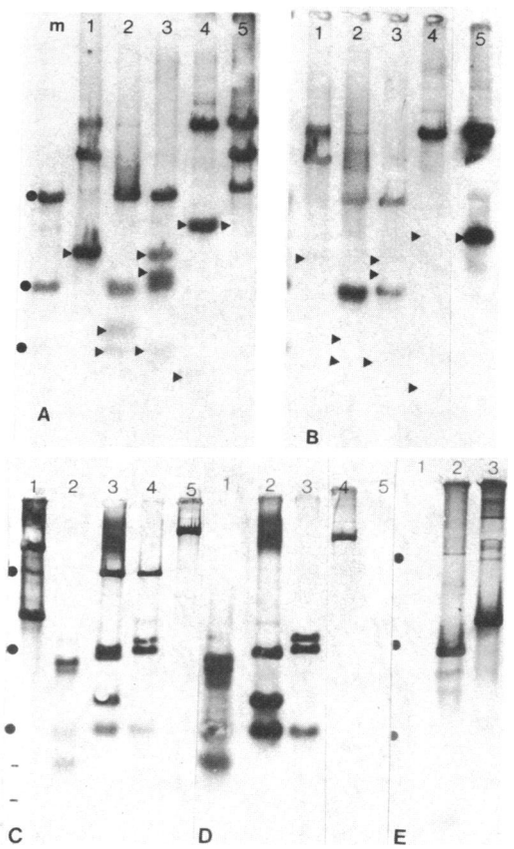

FIG. 2. Cloned cDNAs (Scr-1, GFAP, and neurofilament) tested for sequence homology on Southern blots. (*A*) Representative restriction digests of each clone hybridized to ^{32}P-labeled GFAP plasmid. (*B*) Parallel digests probed with ^{32}P-labeled neurofilament plasmid. Arrowheads denote position of insert fragments resolved from plasmid DNAs. Lane m, marker pUC18 plasmid digested with *Rsa* I giving fragments of 1769, 676, and 241 base pairs (circles in all other blots). Lanes: 1, Scr-1 plasmid DNA digested with *Eco*RI (a single band at arrowhead represents the entire insert); 2, Scr-1 plasmid digested with *Rsa* I; 3, GFAP plasmid digested with *Rsa* I; 4, GFAP plasmid digested with *Hin*dIII; 5, neurofilament plasmid digested with *Eco*RI. Note ^{32}P-labeled GFAP clone hybridizes to Scr-1 insert (lanes 1 and 2) but not to the neurofilament insert (arrowhead, lane 5). ^{32}P-labeled neurofilament plasmid in *B* hybridizes only with plasmid fragments in Scr-1 and GFAP lanes, but highlights its own insert (lane 5, arrowhead). (*C–E*) Representative hybridizations of isolated restriction fragments labeled with biotin-11-dUTP (Bethesda Research Laboratories). (*C*) GFAP 3761 *Hin*dIII fragment (noncoding 3′ region with some plasmid DNA) hybridizes to the Scr-1 insert (see Fig. 3 maps). (*D*) The *Eco*RI Scr-1 insert was used as a probe and is comparable to *C*. (*E*) The 1269 *Hin*dIII GFAP fragment containing only the α-helical coding region does not hybridize to the Scr-1 insert. Lanes: 1 in *C* and *E*, Scr-1 plasmid digested with *Eco*RI; 2 in *C* and 1 in *D*, Scr-1 insert digested with *Hae* III; 3 in *C* and 2 in *D*, Scr-1 plasmid digested with *Rsa* I; 4 in *C*, 3 in *B*, and 2 in *E*, GFAP plasmid digested with *Rsa* I; 5 in *C*, 4 in *D*, and 3 in *E* are GFAP plasmid digested with *Hin*dIII; 5 in *D* is neurofilament plasmid digested with *Eco*RI. Isolated insert probes are demonstrably free of plasmid DNA (lanes 5 in *D* and 1 in *E*). Prior to detection with strepavidin–biotin complexes (11), nylon filters were blocked in 3% (wt/vol) bovine serum albumin in 0.3 M NaCl/0.2 M Tris·HCl, pH 7.5, at 65°C for 1 hr.

In CJD, the increase in GFAP is apparent only subsequent to the mRNA accumulation. Thus at 99 days after inoculation, when cerebral GFAP mRNA levels had already increased 2-fold, anti-GFAP binding was comparable to that seen in control brains. This temporal discrepancy could be simply the consequence of different sensitivities between the two assays. However, 5-fold elevations of GFAP mRNA in the cerebrum

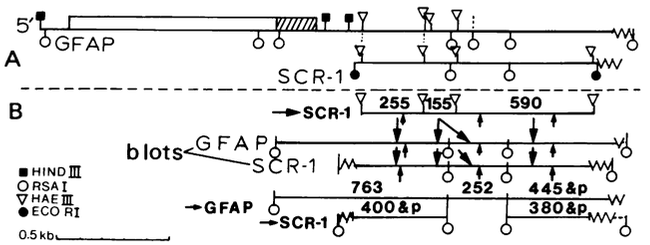

FIG. 3. Summary restriction map (*A*) of GFAP (14) and corresponding Scr-1 homologous sequence regions with key restriction sites. Open bar in GFAP map denotes amino acid coding region, which as shown in Fig. 2 does not contain regions of homology to Scr-1. One putative *Rsa* I site in the GFAP sequence (14) was not detected enzymatically (dotted lines). Two potential GFAP *Hae* III sites (dotted) correspond to detected Scr-1 *Hae* III sites. (*B*) Summary of essential hybridization experiments used for placement of Scr-1 with respect to GFAP. Labeled isolated fragments, bold numbers; downward arrows, positive hybridization of *Hae* III Scr-1 insert fragments; upward arrows, positive hybridizations of GFAP and/or Scr-1 *Rsa* I probe fragments.

(day 111) were associated with readily detectable increases in GFAP immunoreactivity, whereas GFAP was only minimally increased in the cerebellum with comparable 5-fold mRNA elevations. The somewhat increased delay in GFAP accumulation in the cerebellum is similar to the delay in obvious accumulations of myelin basic protein subsequent to mRNA elevations in viral-induced demyelination and remyelination (17). Immunoblot studies of cerebrum GFAP were consistent with immunocytochemical studies, and detailed evaluations of GFAP by immunoblots at terminal stages of disease have been confirmed (D. Dormont, personal communication).

The most striking feature of the regulation of GFAP gene expression during the course of CJD infection is the spatial discontinuity of the destructive neuronal lesions and stimulation of the astrocytes. The degeneration of neurons and their processes, which constitute the spongiform lesions, would be expected to evoke a characteristic increase in mRNA and in plump GFAP-containing astrocytes in the immediate vicinity over a 2- to 3-week period after damage. GFAP mRNA elevations preceded more severe spongiform lesions in the cerebrum (Table 1), and GFAP was not always markedly increased in cerebral regions showing obvious spongiform changes (Fig. 4*D*). Although at the terminal stages of disease there were focal regions with gliosis that could be secondary to neuronal damage (Fig. 4*E*), other cerebral regions revealed a disproportionate increase in GFAP immunoreactivity with respect to neuronal pathology (Fig. 4*C*). Fig. 5 shows that GFAP antibodies specifically decorated glial filaments. Finally, stimulation of astrocytes without neuronal damage is definitively shown in the cerebellum where there were marked increases in GFAP mRNA without any recognizable spongiform lesions by light and electron microscopy (Table 1). The RNA gel blots shown here appear to be more powerful than protein studies as they delineate quantitative changes in all samples prior to more complex pathological sequelae.

In most strains of scrapie [with the exception of strain 263K in hamsters (19)], there is an initial lag in the replication of agent in brain, followed by an exponential increase in infectious titer, which can plateau at late stages of disease. The induction of GFAP could parallel the amount of infectious agent, and stimulation of GFAP gene expression in regions or at times where there is minimal neuronal damage may be more closely related to the presence of the agent than to the neuronal destruction caused by the agent. We therefore assayed the infectivity of normal-appearing cerebellum at clinical stages of disease (120 days) when GFAP mRNA was elevated. Infectivity was significant, with a titer of 7.7 ± 0.2 logarithmic units/g of

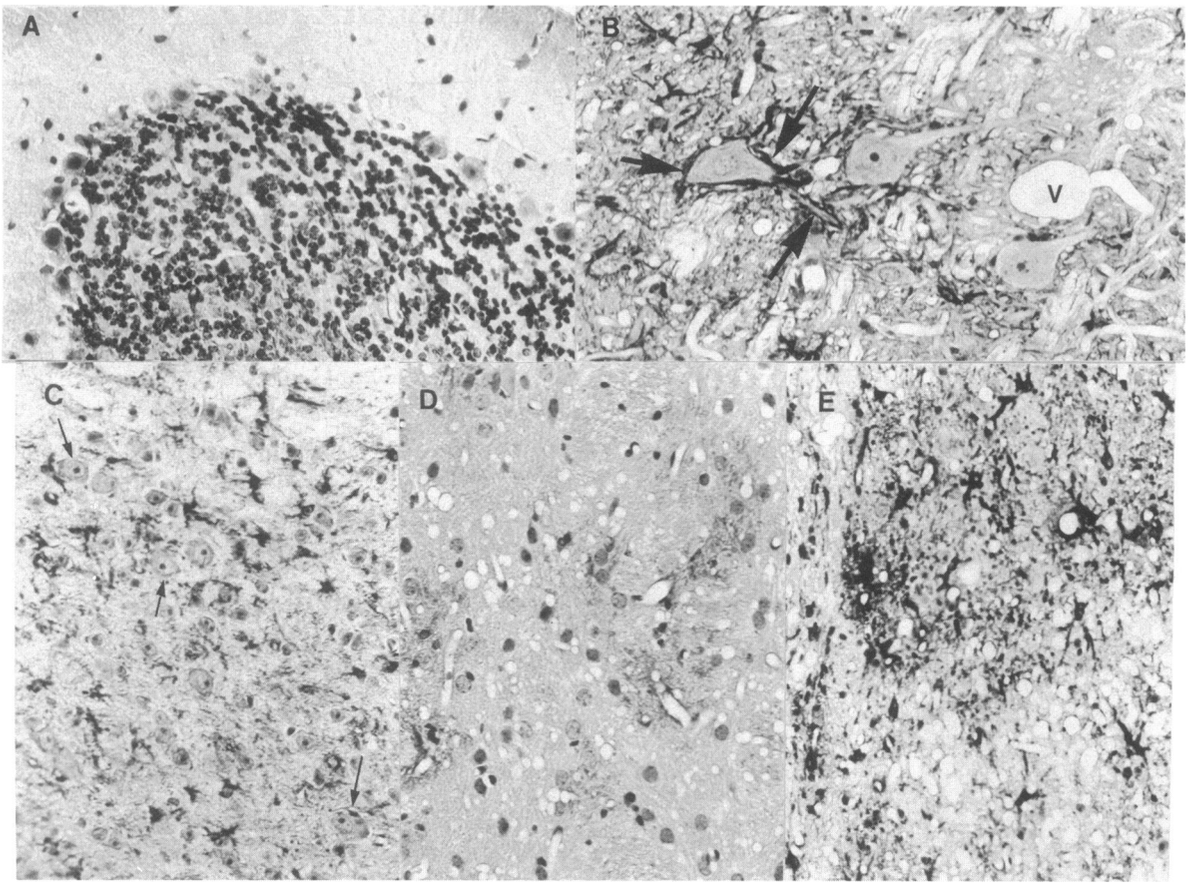

FIG. 4. Immunological detection of GFAP in CJD infected brains. (*A*) Typical terminal cerebellar sampled showing good preservation of Purkinje neurons, no spongiform changes, and negligible GFAP protein accumulation. A few delicate GFAP-positive fibers (normal Bergmann glia) were noted at higher power in the molecular layer, and there was a slight increase in GFAP in deep white matter without spongiform changes (data not shown). (*B*) At 133 days after inoculation, CJD brainstem shows accumulation of GFAP in astrocyte surrounding a well-preserved large neuron and its dendrites (arrows). Large vacuole (V) without surrounding GFAP protein, by shape and from previous electron microscopic studies, probably represents a degenerated large neuron. (*C*) At 111 days after inoculation, CJD cortex shows abundant (darkly stained) GFAP accumulation in astrocytes, well-preserved neurons (e.g., arrows), and an absence of significant spongiform changes. (*D*) Terminal CJD cerebrum (133 days) showed region with obvious spongiform changes without significant GFAP accumulation. (*E*) At 133 days after inoculation, CJD cerebrum with complex focal lesion showing both spongiform changes and concurrent GFAP accumulation in astrocytes. Perfusion with 4% (wt/vol) paraformaldehyde/1% glutaraldehyde in buffer; 4-μm paraffin sections were treated with anti-GFAP antibody and peroxidase-tagged secondary antibody, then counterstained with hematoxylin. (×250 for *A*, *C*, *D*, and *E*; ×500 for *B*.)

cerebellum, which represents ≈25% of cerebral infectivity (8.3 logarithmic units/g) (11) at comparable times and as assayed in this passage at 120 days. Thus a high concentration of infectious agent appears to be responsible for the stimulation of astroglia in this model. Indeed, accumulation of GFAP mRNA appears to be a more accurate predictor than spongiform changes of the spatial and temporal accumulation of the CJD agent within the central nervous system.

Table 1. GFAP mRNA and histopathology

Days after inoculation	Cerebellum		Cerebrum	
	mRNA	Pathology	mRNA	Pathology
87	1	None	1.5	None–RF
99	1.3	None	2	None–RF
111	2	None	5	MF
122	4.5	None	13	SF
133	6	None	13	SF

GFAP mRNA was determined by densitometry of RNA gel blots and the relative amount of mRNA was determined. Histopathology in this hamster CJD model shows focal spongiform changes predominantly in the cortex, yet other large gray structures of the cerebrum (e.g., thalamus) display negligible changes even at terminal stages of disease. Abbreviations for spongiform changes are as follows: RF, rare focal; MF, moderate focal; SF, severe focal change. Parallel animals sacrificed at 120 days showed significant infectivity in both regions.

The exact molecular pathway for GFAP mRNA induction by the CJD agent is unknown. Because the highest titers of infectivity are present in synaptosomal and membrane-rich CJD or scrapie fractions (20–22), it is possible that an agent-specific protein acts directly at the astrocyte membrane to stimulate gene expression. The induction of Ia antigens on astrocytes by a specific glycoprotein of the mouse hepatitis virus is an example of this type of regulation (23). Although no viral protein has been identified in CJD (11), a host membrane protein (2, 24), which can be proteolytically cleaved to form amyloid-like fibrils specific for unconventional viral agents (21, 25, 26) especially at late stages of disease (27), could provide an analogous signal for astrocytic hypertrophy. More subtle functional alterations in host cell membranes (28) could also lead to the generation of a signal that directly stimulates adjacent astrocytes.

Persistent viral infections in the brain show similarities to the spatial and temporal accumulation of specific glial mRNAs and/or proteins demonstrated here, and these stimulations have been attributed to the production of diffusible factors (17, 29). In persistent lymphocytic-choriomeningitis, viral antigen-stimulated perivascular lymphocytes are thought to produce a lymphokine that diffuses throughout the brain parenchyma and stimulates GFAP synthesis as part of a pleiotrophic response

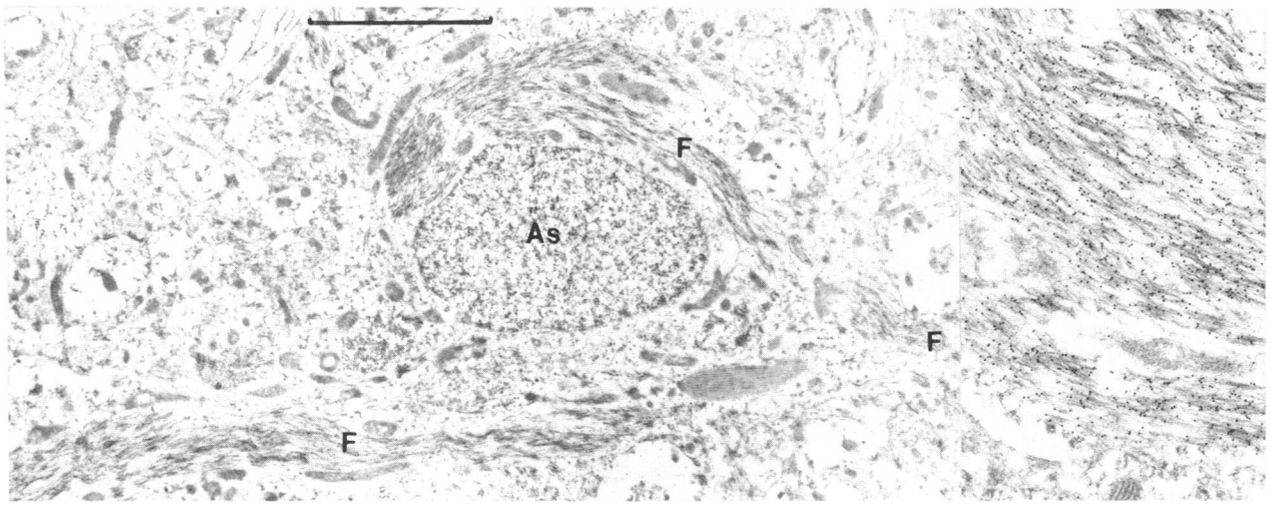

FIG. 5. Typical hypertrophic astrocyte in CJD (133 days) with accumulated GFAP fibrils clearly bind GFAP antibodies (representatively shown at high magnification at right); primary antibody was detected with 10-nm gold-protein A, and tissue was embedded in LR white (without osmification) for antigen detection (18). Background was 0–10 gold particles per 5 μm^2, and all GFAP filaments observed were labeled. (Bar = 1 μm.)

(29). Similarly, GFAP can accumulate in regions devoid of lesions in allergic encephalomyelitis (30). Because there is no lymphocytic response in CJD, a humoral factor in CJD would have to derive from nonlymphocytic brain cells, e.g., astrocytes, microglia, or endothelial cells. Interleukin 1, known to be involved in viral infections of the central nervous system, is produced at high levels by astroglia, microglia, and endothelial cells (31). Often several regulatory peptides can act in concert or have similar effects.

The involvement of a diffusible factor in CJD receives support from our studies of cell lines derived from CJD infected brain or exposed to CJD *in vitro* (32–34). These nonlymphocytic cells produce peptide growth factors, including a TGF-α-like activity, which is capable of stimulating GFAP gene expression in indicator astrocytic cells (E. Oleszak, G. Murdoch, L.M., and E.E.M., unpublished observations). In these *in vitro* models the agent could mediate growth factor production either through insertional mutagenesis or production of a trans-acting transcriptional activator, as several studies suggest that the CJD agent has biological properties similar to slowly oncogenic retroviruses (32–34). The study of regulatory peptides in CJD and their effects on gene expression in brain may elucidate pathways common to several types of dementia (26).

We thank Ashley Haase for his generous gift of the Scr-1 cDNA clone and Nick Cowan for the neurofilament and GFAP cDNA clones. W. Fritch and C. Coady graciously assisted with animal inoculations and histological preparations. This work was supported by Grants NS 12674 and AG 03106 from the National Institutes of Health.

1. Gajdusek, D. C. (1977) *Science* **197,** 943–960.
2. Manuelidis, L. & Manuelidis, E. E. (1986) *Prog. Med. Virol.* **33,** 78–98.
3. Manuelidis, E. E. & Manuelidis, L. (1979) in *Slow Transmissible Diseases of the Nervous System*, eds. Prusiner, S. B. & Hadlow, W. J. (Academic, New York), Vol. 2, pp. 147–173.
4. Manuelidis, E. E., Gorgacz, E. J. & Manuelidis, L. (1978) *Science* **200,** 1069–1071.
5. Kim, J. H. & Manuelidis, E. E. (1986) *Acta Neuropathol.* **69,** 81–90.
6. Manuelidis, E. E., Manuelidis, L., Pincus, J. H. & Collins, W. F. (1978) *Lancet* **ii,** 40–42.
7. Manuelidis, E. E., Gorgacz, E. J. & Manuelidis, L. (1978) *Proc. Natl. Acad. Sci. USA* **75,** 3432–3436.
8. Chirgwin, J. M., Przybyla, A. E., MacDonald, R. J. & Rutter, W. J. (1979) *Biochemistry* **18,** 5294–5299.
9. Feinberg, A. P. & Vogelstein, B. (1983) *Anal. Biochem.* **132,** 6–13.
10. Reed, K. C. & Mann, D. A. (1985) *Nucleic Acids Res.* **13,** 7207–7221.
11. Manuelidis, L., Sklaviadis, T. & Manuelidis, E. E. (1987) *EMBO J.* **6,** 341–342.
12. Weitgrefe, S., Zupancic, M., Haase, A., Chesebro, B., Race, R., Frey, W., Rustan, T. & Friedman, R. L. (1985) *Science* **230,** 1177–1179.
13. Lewis, S. A. & Cowan, N. J. (1985) *J. Cell Biol.* **100,** 843–850.
14. Lewis, S. A., Balcarek, J. M., Krek, V., Shelanski, M. & Cowan, N. J. (1984) *Proc. Natl. Acad. Sci. USA* **81,** 2743–2746.
15. Manuelidis, L. & Manuelidis, E. E. (1974) *Exp. Neurol.* **43,** 192–206.
16. Kimberlin, R. H. (1976) in *Slow Virus Diseases of Animals and Man*, ed. Kimberlin, R. H. (North-Holland, Amsterdam), pp. 307–323.
17. Kristensson, K., Holmes, K. V., Duchala, C. S., Zeller, N. K., Lazzarini, R. A. & Dubois-Dalcq, M. (1986) *Nature (London)* **322,** 544–547.
18. Graber, M. B. & Kreutzberg, G. W. (1985) *Histochemistry* **83,** 497–500.
19. Kimberlin, R. H. & Walker, C. A. (1986) *J. Gen. Virol.* **67,** 2005–2009.
20. Manuelidis, L. & Manuelidis, E. E. (1983) *Banbury Rep.* **15,** 399–412.
21. Manuelidis, L., Valley, S. & Manuelidis, E. E. (1985) *Proc. Natl. Acad. Sci. USA* **82,** 4263–4267.
22. Somerville, R. A., Merz, P. A. & Carp, R. I. (1986) *Intervirology* **25,** 48–55.
23. Massa, P. T., Dorries, R. & terMeulen, V. (1986) *Nature (London)* **320,** 543–546.
24. Prusiner, S. B. (1984) *Cell* **38,** 127–139.
25. Brown, P., Coker-Vann, M., Pomeroy, K., Franko, M., Asher, D., Gibbs, C. J. & Gajdusek, D. C. (1986) *N. Engl. J. Med.* **314,** 547–551.
26. Manuelidis, L., Sklaviadis, T. & Manuelidis, E. E. (1987) in *Second Symposium on Non-conventional Viruses of the Central Nervous System*, ed. Court, L. (Masson, Paris), in press.
27. Czub, M., Braig, H. R. & Diringer, H. (1986) *J. Gen. Virol.* **67,** 2005–2009.
28. Rasenick, M. M., Valley, S., Manuelidis, E. E. & Manuelidis, L. (1986) *FEBS Lett.* **198,** 164–168.
29. Oldstone, M. B. A., Blount, P., Southern, P. J. & Lampert, P. W. (1986) *Nature (London)* **321,** 239–243.
30. Smith, M. E., Somera, F. P. & Eng, L. F. (1983) *Brain Res.* **264,** 241–253.
31. Dinarello, C. A. (1986) in *Year in Immunology*, eds. Cruse, J. M. & Lewis, R. E. (Karger, New York), Vol. 2, pp. 68–69.
32. Manuelidis, E. E. & Manuelidis, L. (1983) *Banbury Rep.* **15,** 413–424.
33. Oleszak, E., Manuelidis, L. & Manuelidis, E. E. (1986) *J. Neuropathol. Exp. Neurol.* **45,** 489–502.
34. Manuelidis, E. E., Fritch, W. W., Kim, J. H. & Manuelidis, L. (1987) *Proc. Natl. Acad. Sci. USA* **84,** 871–875.